Research Journal of Applied Sciences, Engineering and Technology 4(20): 4055-4065, 2012
ISSN: 2040-7467

Submitted: March 07, 2012 Accepted: March 16, 2012 Published: October 15, 2012

Free and Forced Vibrations of FGM Conical Shell Under Impulse Loads

[1]Amirhossein Nezhadi, [1]Roslan Abdul Rahman, [1]Amran Ayob and [2]Keramat Malekzadeh Fard
[1]Faculty of Mechanical Engineering, Universiti Teknologi Malaysia (UTM), 81310 Skudai, Johor, Malaysia
[2]Department of Structural Analysis, Space Research Center, 26th Kilometer of Expressway of Tehran-Karaj, Tehran, Iran

Abstract: In this study, an effective method for analyzing the forced vibration of FG conical shell under impulse loads is presented. A set of simpler principal vibration modes of conical shell are presented which satisfies the end boundary conditions of simply supported. The modulus of elasticity and mass density of Functionally Graded (FG) conical shell is assumed to vary according to a gradient index in terms of the volume fractions of the constituents. The Rayleigh-Ritz method with Hamilton's principle is used to obtain the equation of motion of functionally graded conical shell. By solving eigenvalue problem of the equation of motion, the natural frequencies and the dynamic responses of functionally graded conical shell can be calculated. The considered impulse load types are step pulse, sine pulse, triangular pulse and exponential pulse. To validate the present analysis, numerical comparisons between results with those in the literature and calculated by the software ABAQUS are done.

Keywords: Conical shell, forced vibration, functionally graded materials, impulse load

INTRODUCTION

A group of materials scientists in Japan introduced the idea of the construction of functionally graded materials in 1984. FGMs have experienced a remarkable increase in terms of development and research programs during the past two decade. World wide dissemination and distribution of the results through international meetings, exchange programs and publications testifies to this increasing growth. They have obtained many applications in space plan body, rocket engine components, nuclear reactor components, engine components, first wall of fusion reactor, hip implant, turbine blades and other technological and engineering applications. A detailed discussion on their applications, processing and design can be found in Refs. Obata and Noda (1996), Wetherhold *et al*. (1996), Suresh and Mortensen (1998), Miyamoto *et al*. (1999) and Kieback *et al*. (2003). Commonly, FGMs are made from a mixture of ceramics and metals and are more characterized by a continuous and smooth change of the mechanical properties from one surface to another. In addition, a mixture of ceramic and metal with a continuously changing volume fraction can be easily fabricated. (Reddy and Chin, 1998; Liew *et al*., 2002). FGMs now have been considered as one of the most promising candidates for future smart composites in numerous engineering fields. Most of FGMs and composite shells are used under impulse load and application of this loading may cause strength reduction and large deformation. Regarding the obvious significance in practical applications, the dynamic responses of the structure in design process have attracted many research efforts. Between those available, Christoforou and Swanson (1990) gave an analytic solution for the problem of simply-supported orthotropic cylindrical shells subject to impact loading. Lee and Lee (1997) used the first-order shear deformation shell theory to investigate the free vibration and dynamic response for the CFRP and GFRP cross-ply laminated circular cylindrical shells under impulse loads. Matemilola and Stronge (1997) developed an analytical solution for the impact response of a simply supported anisotropic composite cylinder. Sofiyev *et al*. (2009) used the Galerkin method to investigate the vibration and stability of orthotropic conical shells under a hydrostatic pressure. Furthermore, Fares *et al*. (2004) studied the problem of minimizing the dynamic response of laminated truncated conical shells with minimum control force is studied. Sofiyev (2004) presented the stability of FG conical shells subject to aperiodic impulsive loading has been presented. Jafari *et al*. (2005) used the first-order shear deformation shell theory to investigate free and forced vibration of composite circular cylindrical shells under radial impulse load and axial compressive loads.

Khalili *et al*. (2009) investigated free and forced vibration of multilayer composite circular cylindrical

Corresponding Author: Amirhossein Nezhadi, Faculty of Mechanical Engineering, Universiti Teknologi Malaysia, 81310 Skudai, Johor, Malaysia

shells under transverse impulse load as well as combined static axial loads and internal pressure based on first order shear deformation theory. Malekzadeh *et al*. (2010) studied dynamic response of multilayer circular cylindrical shells formed from hybrid composite materials under lateral impulse load is studied. Despite the fact that many studies on the dynamic problems of the conical and cylindrical shells have been published, the forced vibration problems of the FG conical shell under impulse loads have to be comprehensively studied. Through dynamic response analysis, an efficient way for computing the forced vibration responses can be obtained and further used in the vibration control and dynamic designs of the conical shells. The Rayleigh-Ritz method is used because the equation of motion of FG conical shell is very complicated that makes it difficult to analytically solve it. In this study, free and forced vibration of conical shell made of Functionally Gradient Material (FGM) under impulse loads is investigated by using the Rayleigh-Ritz method.

METHDOLOGY

Functionally gradient materials: In which for functionally graded materials with two constituent materials, Poisson ratio υ is assumed to be constant through the thickness, whereas the variations through the thickness of Young's modulus E(η) and the mass density per unit volume ρ(η) can be written as (Matsunaga, 2009):

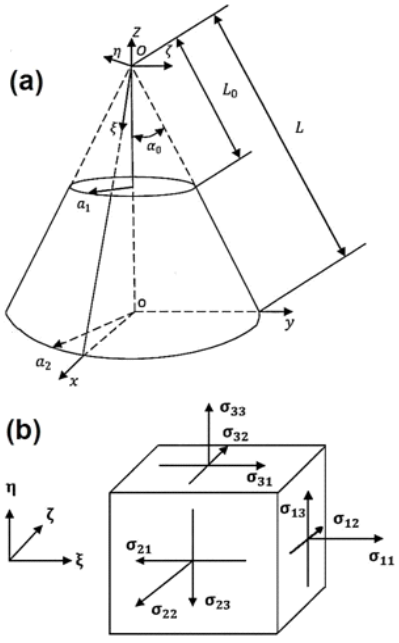

Fig. 1: The schematic diagram of a FGM conical shell (a) The geometry and the curvilinear surface and cartesian coordinate systems; (b) The infinitesimal shell element and the corresponding stresses

$$E(\eta) = E_M + (E_C - E_M)(0.5 + \eta/h)^p \quad (1)$$

$$\rho(\eta) = \rho_M + (\rho_C - \rho_M)(0.5+\eta/h)^p \quad (2)$$

where η is the thickness coordinate ($-h/2 \le \eta \le h/2$), and $p \ge 0$ is the gradient index. Subscripts C and M refer to the ceramic and metal constituents, respectively. For the value p = 0, a fully ceramic shell is intended and infinite p, a fully metallic shell. When the gradient index is increased, the content of metal in the FGM layers decreased.

Equation of motion of functionally graded conical shell: A thin and FG conical shell with constant thickness is assumed. Figure 1 shows the schematic diagram of the conical shell. The two boundaries of the conical shell are Simply Supported (S-S). The corresponding curvilinear surface coordinates O - ξζη and Cartesian coordinates O-xyz are also shown in Fig. 1. The curvilinear surface coordinates are limited to be orthogonal ones which coincide with the lines of principal curvature of the neutral surface. For conical shells, the lines of principal curvature of the neutral surface are the circles (ζ-axis) and parallel meridians (ξ-axis). For a thin conical shell, plane stress condition is assumed and the constitutive relation is given by:

$$\{\sigma\} = [Q]\{e\} \quad (3)$$

where {σ} is the stress vector, {e} is the strain vector and [Q] is the reduced stiffness matrix. The stress vector and the strain vector are defined as:

$$\{\sigma\}^T = \{\sigma_{11}\ \sigma_{22}\ \sigma_{12}\ \sigma_{23}\} \quad (4)$$

$$\{e\}^T = \{\varepsilon_{11}\ \varepsilon_{22}\ \varepsilon_{12}\ \varepsilon_{23}\} \quad (5)$$

where, ε_{ij} (i, j = 1, 2, 3)are the strains and σ_{ij}(i, j = 1, 2, 3) are the stresses in which 1, 2 and 3 coincide with the ξ,ζ and η directions. Where σ_{11} and σ_{22} are the normal stresses acting in the ξ and ζ directions, σ_{12} and σ_{22} are the shear stresses in the curvilinear coordinate O - ξζη as shown in Fig. 1b. The reduced stiffness matrix is defined as:

$$[Q] = \begin{bmatrix} Q_{11} & Q_{12} & 0 & 0 \\ Q_{12} & Q_{22} & 0 & 0 \\ 0 & 0 & Q_{66} & 0 \\ 0 & 0 & 0 & Q_{66} \end{bmatrix} \quad (6)$$

For FGM materials the reduced stiffness Q_{ij}(i, j = 1, 2 and 6, respectively) are defined as:

$$Q_{11} = Q_{22} = \frac{E(\eta)}{(1-\mu^2)} \quad Q_{12} = \frac{\mu E(\eta)}{(1-\mu^2)}$$
$$Q_{66} = \frac{E(\eta)}{2(1+\mu)} \quad (7)$$

where is the Young's modulus and μ is the Poisson's ratio. According Soedel (2004), the components in the strain vector {e} are defined as:

$$\varepsilon_{11} = e_1 + \eta k_1 \qquad \varepsilon_{22} = e_2 + \eta k_2$$
$$\varepsilon_{12} = \gamma + 2\eta\tau \qquad \varepsilon_{23} = e_{23} \tag{8}$$

where e_1,e_2,γ and e_{23} are the references surface strains, and k_1,k_2 and τ are the surface curvatures. These surface strains and curvatures are defined as:

$$e_1 = \frac{\partial u}{\partial \xi} \qquad e_2 = \frac{1}{\xi \sin\alpha_0}\frac{\partial v}{\partial \zeta} + \frac{u}{\xi} + \frac{w}{\xi \tan\alpha_0}$$

$$\gamma = \frac{1}{\xi \sin\alpha_0}\frac{\partial u}{\partial \zeta} + \frac{\partial v}{\partial \xi} - \frac{v}{\xi} \qquad e_{23} = \frac{v}{\xi \tan\alpha_0}$$

$$k_1 = -\frac{\partial^2 w}{\partial \xi^2}$$

$$k_2 = \frac{1}{\xi^2 \sin\alpha_0 \tan\alpha_0}\frac{\partial v}{\partial \zeta} - \frac{1}{\xi^2 \sin^2\alpha_0}\frac{\partial^2 w}{\partial \zeta^2} - \frac{1}{\xi}\frac{\partial w}{\partial \xi}$$

$$\tau = -\frac{1}{\xi \sin\alpha_0}\frac{\partial^2 w}{\partial \xi \partial \zeta} + \frac{1}{2\xi \tan\alpha_0}\frac{\partial v}{\partial \xi} - \frac{1}{\xi^2 \tan\alpha_0}v$$

$$+ \frac{1}{\xi^2 \sin\alpha_0}\frac{\partial w}{\partial \zeta} \tag{9}$$

For a thin conical shell the force and moment resultants are defined as:

$$\left\{N_\xi, N_\zeta, N_{\xi\zeta}, N_{\zeta\eta}\right\} = \int_{-h/2}^{h/2}\left\{\sigma_{11}, \sigma_{22}, \sigma_{12}, \sigma_{23}\right\}d_\eta, \tag{10}$$

$$\left\{M_\xi, M_\zeta, M_{\xi\zeta}\right\} = \int_{-h/2}^{h/2}\left\{\sigma_{11}, \sigma_{22}, \sigma_{12}\right\}\eta\, d_\eta, \tag{11}$$

Substituting Eq. (3), with substitution from Eq. (8), into (10) and (11), the constitutive equation is obtained as:

$$\{N\} = [S]\{\varepsilon\} \tag{12}$$

where, {N} and {ε} and [S] are, respectively, defined as:

$$\{N\}^T = \{N_\xi\ N_\zeta\ N_{\xi\zeta}\ N_{\zeta\eta}\ M_\xi\ M_\zeta\ M_{\xi\zeta}\} \tag{13}$$

$$\{\varepsilon\}^T = \{e_1\ e_2\ \gamma e_{23}\ k_1\ k_2\ 2\tau\} \tag{14}$$

$$[s] = \begin{bmatrix} A_{11} & A_{12} & 0 & 0 & B_{11} & B_{12} & 0 \\ A_{12} & A_{22} & 0 & 0 & B_{12} & B_{22} & 0 \\ 0 & 0 & A_{66} & 0 & 0 & 0 & B_{66} \\ 0 & 0 & 0 & A_{66} & 0 & 0 & 0 \\ B_{11} & B_{12} & 0 & 0 & D_{11} & D_{12} & 0 \\ B_{12} & B_{22} & 0 & 0 & D_{12} & D_{22} & 0 \\ 0 & 0 & B_{66} & 0 & 0 & 0 & D_{66} \end{bmatrix} \tag{15}$$

where A_{ij}, B_{ij} and D_{ij} (i, j = 1, 2 and 6) are the extensional, coupling and bending stiffnesses defined as:

$$\left\{A_{ij}, B_{ij}, D_{ij}\right\} = \int_{-h/2}^{h/2} Q_{ij}\left\{1, \eta, \eta^2\right\}d_\eta \tag{16}$$

when the reduced stiffness matrixes are a function of η for functionally gradient materials, B_{ij} are present in the constitutive equation for a FG conical shell, unlike a homogeneous isotropic conical shell where the B_{ij} do not exist.

To determine the equation of motion of the conical shell, Hamilton's principle with the Rayleigh-Ritz method will be used. Hamilton's principle is written by Soedel (2004):

$$\int_{t_1}^{t_2}\delta(T - U)dt + \int_{t_1}^{t_2}\delta W dt = 0 \tag{17}$$

where, T the kinetic energy, U strain energy and W work, t_1 and t_2 are the integration time limits, δ(0) denotes the first variation. The strain energy and kinetic energy and virtual work of a conical shell can be written as:

$$T = \frac{1}{2}\int_{-h/2}^{h/2}\int_0^{2\pi}\int_{L_o}^{L}\rho(\eta)\left[\left(\frac{\partial u}{\partial t}\right)^2 + \left(\frac{\partial v}{\partial t}\right)^2 + \left(\frac{\partial w}{\partial t}\right)^2\right] \tag{18}$$
$$\xi \sin\alpha_0 d_\xi d_\zeta d_\eta$$

$$U = \frac{1}{2}\int_{-h/2}^{h/2}\int_0^{2\pi}\int_{L_0}^{L}\{\varepsilon\}^T[S]\{\varepsilon\}\xi \sin\alpha_0 d_\xi d_\zeta d_\eta \tag{19}$$

$$\delta W = \int_0^{2\pi}\int_{L_0}^{L}\left(q_1\delta u + q_2\delta v + q_3\delta w\right)\xi \sin\alpha_0 d_\xi d_\zeta \tag{20}$$

where, q_1, q_2, and q_3 are the distributed load components per unit area along the ξ, ζ and η directions and are assumed to act on the neutral surface of the shell. The units of q_1,q_2 and q_3 are [N/m^2].

The distributed loads $q_1(t)$, $q_2(t)$ are equal to zero and the FG conical shell subjected to distributed radial load of $q_3(t)$ per unit area on a localized small patch bounded by $-\zeta_1 \le \zeta \le \zeta_1$ and $((L+L_0)/2)-L_2) \le \xi \le ((L+L_0)/2)+L_2)$ that they are written by:

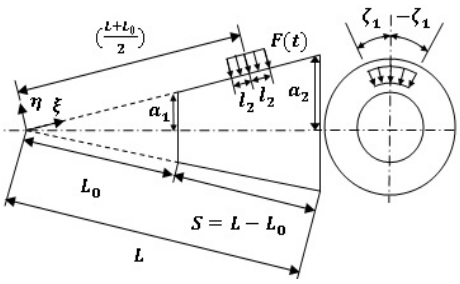

Fig. 2: Distributed load over small area

$$q_1(t) = 0, q_2(t) = 0, q_3(t) = \sum_{i=1}^{m}\sum_{j=1}^{n} q_{30} F_{ij}(t) \qquad (21)$$

q_{30} is the amplitude. Substituting Eq. (21) into (20), The work done by this load on the conical shell is (Kandasamy, 2008):

$$\delta W = \int_{-\zeta_1}^{\zeta_1}\int_{\frac{L+L_0}{2}-L_2}^{\frac{L+L_0}{2}+L_2}\left(q_3\delta w\right)\xi\sin\alpha_0 d_\xi d_\zeta \qquad (22)$$

For simply supported conical shell, the boundary conditions at both ends can be written as:

$$v = w = N_{11} = M_{11} = 0 \qquad (23)$$

at $\xi = 1$ and $\xi = 1_0$ would be considered. In the Rayleigh-Ritz method, the shape of deformation of the continuous system is approximated using a series of trial shape functions that must satisfy the geometric boundary conditions. The displacements can be written as:

$$u(\xi,\zeta,t) = \sum_{i=1}^{m}\sum_{j=1}^{n} U_{ij}(\xi,\zeta)p_{ij}(t) = U^T(\xi,\zeta)P(t) \qquad (24)$$

$$v(\xi,\zeta,t) = \sum_{i=1}^{m}\sum_{j=1}^{n} V_{ij}(\xi,\zeta)r_{ij}(t) = V^T(\xi,\zeta)r(t) \qquad (25)$$

$$w(\xi,\zeta,t) = \sum_{i=1}^{m}\sum_{j=1}^{n} W_{ij}(\xi,\zeta)s_{ij}(t) = W^T(\xi,\zeta)s(t) \qquad (26)$$

where, U, V and W are the trial shape functions or the principal vibration modes, and p, r, s are the generalized coordinates or modal coordinates. They are defined as:

$$p = [p_{11}, \ldots, p_{1n}, p_{21}, \ldots, p_{2n}, p_{m1}, \ldots, p_{mn}]^T$$
$$r = [r_{11}, \ldots, r_1 n, r_{21}, \ldots, r_{2n}, r_{m1}, \ldots, r_{mn}]^T$$
$$s = [s_{11}, \ldots, s_1 n, s_{21}, \ldots, s_{2n}, s_{m1}, \ldots, s_{mn}]^T$$
$$U = [U_{11}, \ldots, U_{1n}, U_{21}, \ldots, U_{2n}, U_{m1}, \ldots, U_{mn}]^T$$
$$V = [V_{11}, \ldots, V_{1n}, V_{21}, \ldots, V_{2n}, V_{m1}, \ldots, V_{mn}]^T$$
$$W = [W_{11}, \ldots, W_{1n}, W_{2n}, \ldots, W_{m1}, \ldots, W_{mn}]^T \qquad (27)$$

It is necessary to demonstrate the formulations of the principle mode shapes U, V and W in Eq. (24)-(26). A number of vibration mode shapes of conical shells have been utilized. According a number of researches, (Soedel, 2004; Shabana, 1997; Clough and Penzien, 1993), the displacement field is approximated using a series of trial shape functions that must satisfy the geometric boundary conditions of the problem. For instance, references Li (2000) and Lam and Li (1999) used a kind of vibration modes of conical shells that are similar to those of cylindrical shells. The main mode shapes of conical shells with simply supported boundaries can be declared as:

$$U_{ij}(\xi,\zeta) = \cos\left[\frac{i\pi(\xi - 1_0)}{1 - 1_0}\right]\cos(j\zeta)$$

$$V_{ij}(\xi,\zeta) = \sin\left[\frac{i\pi(\xi - 1_0)}{1 - 1_0}\right]\sin(j\zeta) \qquad (28)$$

$$W_{ij}(\xi,\zeta) = \sin\left[\frac{i\pi(\xi - 1_0)}{1 - 1_0}\right]\cos(j\zeta)$$

i = 1, 2, …, m; j = 1, 2, …, n

where, i and j denote the wave numbers in the meridional and circumferential directions. Substituting Eq. (18), (19) and (22) in terms of the generalized coordinates and displacement shape functions into Eq. (17) and fulfilling the variation operation in terms of p, r and s. They can be obtained as:

$$M_t\frac{d^2x}{dt^2} + K_t X = Q \qquad (29)$$

where, M_t the generalized mass matrix, K_t the stiffness matrix, Q the forcing matrix, X the generalized coordinate matrix and written by:

$$M_t = \begin{bmatrix} M_1 & 0 & 0 \\ 0 & M_2 & 0 \\ 0 & 0 & M_3 \end{bmatrix} \qquad K_t = \begin{bmatrix} K_1 & K_2 & K_3 \\ K_2^T & K_4 & K_5 \\ K_3^T & K_5^T & K_6 \end{bmatrix}$$

$$Q = [0\ 0\ Fq_3\ q_3]^T \qquad X = [p^T\ r^T\ s^T]^T \qquad (30)$$

where, M_1,M_2 and M_3 are the modal mass matrices and K_1,K_2,…,K_6 are the modal stiffness matrices and F_{q3} is the forcing matrice which are given in Appendix . A solution of Eq. (29) is in the form:

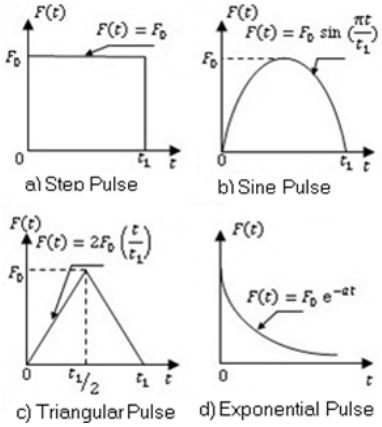

Fig. 3: Considered pulse shapes (a) Step pulse (b) Sine pulse (c) Triangular pulse (d) Exponential pulse

$$X(t) = X_0 e^{\lambda t} \tag{31}$$

where, λ is the characteristic values or the eigenvalue and X_0 is the eigenvector. Substituting Eq. (31) into the homogeneous differential equation of Eq. (29) leads to the following standard eigenvalue problem:

$$(M_t\lambda^2+K_t)X_0 = 0 \tag{32}$$

From which the eignvalues and eignvectors can be obtinethed. The imaginary parts of the eigenvalues are the natural frequencies of the FG conical shell. Substituting Eq. (30) into (29) gives:

$$\ddot{s}_{ij}(t) + \omega_{ij}^2 s_{ij}(t) = \frac{Fq_{3_{ij}}q_3}{M_{3_{ij}}} \tag{33}$$

For zero initial conditions, the solution of Eq. (33) will be:

$$s_{ij}(t) = \frac{Fq_{3_{ij}}q_{30}}{M_{3_{ij}}}\int_0^t F(\tau)\sin\omega_{ij}(t-\tau)d_\tau \tag{34}$$

and the transverse displacement at any point of the shell is given by:

$$w(\xi,\zeta,t) = \sum_{i=1}^{m}\sum_{j=1}^{n}\frac{F_{q3_{ij}}q_{30}}{M_{3_{ij}}}\sin\left[\frac{i\pi(\xi-1_0)}{1-1_0}\right]\cos(j\zeta)\times$$

$$\int_0^t F(\tau)\sin\omega_{ij}(t-\tau)d_\tau \tag{35}$$

Expression of impulse loads: The convolution integral in Eq. (34)-(35) have been solved analytically for different commonly encountered forcing functions:

- Step pulse (Fig. 3a): $F(t) = \begin{cases} F_0, & 0 \le t \le t_1 \\ 0 & t > t_1 \end{cases}$

$$\int_0^t F(\tau)\sin\omega_{ij}(t-\tau)d_\tau =$$

$$\begin{cases} \dfrac{F_0}{\omega_{ij}}(1-\cos\omega_{ij}t) & 0 \le t \le t_1 \\ \dfrac{F_0}{\omega_{ij}}(\cos\omega_{ij}(t-t_1)-\cos\omega_{ij}t), & t > t_1 \end{cases} \tag{36a}$$

- Sine pulse (Fig. 3b):

$$F(t) = \begin{cases} F_0\sin\left(\dfrac{\pi t}{t_1}\right) & 0 \le t \le t_1 \\ 0 & t > t_1 \end{cases}$$

$$\int_0^t F(\tau)\sin\omega_{ij}(t-\tau)d_\tau =$$

$$\begin{cases} \dfrac{F_0 t_1\left[\pi\sin\left(\omega_{ij}t\right)-\omega_{ij}t_1\sin\left(\dfrac{\pi t}{t_1}\right)\right]}{\left(\pi^2-t_1^2\omega_{ij}^2\right)}, & 0 \le t \le t_1 \\ \dfrac{F_0 t_1\pi\left[\sin\left(\omega_{ij}t\right)+\sin\omega_{ij}\left(t-t_1\right)\right]}{\left(\pi^2-t_1^2\omega_{ij}^2\right)}, & t > t_1 \end{cases} \tag{36b}$$

- Triangular pulse (Fig. 3c):

$$F(t) = \begin{cases} 2F_0\left(\dfrac{t}{t_1}\right) & 0 \le t \le \dfrac{t_1}{2} \\ \dfrac{-4F_0\left(t-\dfrac{t_1}{2}\right)}{t_1} & \dfrac{t_1}{2} \le t \le t_1 \\ \dfrac{2F_0(t-t_1)}{t_1} & t > t_1 \end{cases}$$

$$\int_0^t F(\tau)\sin\omega_{ij}(t-\tau)d_\tau =$$

$$\begin{cases} \dfrac{2F_0}{\omega_{ij}}\left[\dfrac{t}{t_1}-\dfrac{\sin(\omega_{ij}t)}{(\omega_{ij}t_1)}\right], & 0\le t\le \dfrac{t_1}{2} \\ \dfrac{2F_0}{\omega_{ij}}\left[1-\dfrac{t}{t_1}-\dfrac{\sin(\omega_{ij}t)}{(\omega_{ij}t_1)}+\dfrac{2\sin\omega_{ij}\left(t-\dfrac{t_1}{2}\right)}{\left(\omega_{ij}t_1\right)}\right], & \dfrac{t_1}{2}\le t\le t_1 \\ \dfrac{2F_0}{\omega_{ij}}\left[\dfrac{-\sin\left(\omega_{ij}t\right)}{\left(\omega_{ij}t_1\right)}+\dfrac{2\sin\omega_{ij}\left(t-\dfrac{t_1}{2}\right)}{\left(\omega_{ij}t_1\right)}-\dfrac{\sin\omega_{ij}(t-t_1)}{(\omega_{ij}t_1)}\right] & \end{cases} \quad (36c)$$

$t > t_1$

- Exponential pulse (Fig. 3d):

$F(t) = F_0e^{-at} \quad 0\le t$

$$\int_0^t F(\tau)\sin\omega_{ij}(t-\tau)d_\tau =$$

$$\begin{cases} \dfrac{F_0\left[\omega_{ij}e^{-at}+a\sin\left(\omega_{ij}t\right)-\omega_{ij}\cos\left(\omega_{ij}t\right)\right]}{\left(a^2+\omega_{ij}^2\right)}, & 0<t\le t_1 \\ \dfrac{F_0\left[e^{-at_1}+\left(\omega_{ij}\cos\omega_{ij}\left(t-t_1\right)-a\sin\omega_{ij}\left(t-t_1\right)\right)\right]}{\left(a^2+\omega_{ij}^2\right)} & \\ \dfrac{F_0\left[\omega_{ij}\cos\left(\omega_{ij}t\right)-a\sin\left(\omega_{ij}t\right)\right]}{\left(a^2+\omega_{ij}^2\right)}, & t>t_1 \end{cases} \quad (36d)$$

RESULTS AND DISCUSSION

Results of free vibration: The results for gradient index p = Infinity (Metal) are compared with the open literature in Table 1. In the numerical calculations, the non-dimensional frequency parameter is defined as Irie *et al*. (1984) and Lam and Li (1999)

$$f = \omega_0\alpha_2\sqrt{\frac{\rho_m(1-\mu^2)}{E_m}} \quad (37)$$

where ω_0 is the natural frequency of the conical shell in radians per second. The material properties used in the present study is:

Metal (Aluminium, Al):

Table 1: Comparisons of frequency parameter f for the conical shell with S-S boundaries (m = 1, p = Infinity (Metal))

	n	Irie et al. (1984)	Lam and Li (1999)	Present
α_0 = 30°	2	0.7910	0.8420	0.84307
	3	0.7284	0.7376	0.74163
	4	0.6352	0.6362	0.64194
	5	0.5531	0.5528	0.55902
	6	0.4949	0.4950	0.50079
	7	0.4653	0.4661	0.47079
	8	0.4654	0.4660	0.46921
	9	0.4892	0.4916	0.49318
α_0 = 45°	2	0.6879	0.7655	0.76424
	3	0.6973	0.7212	0.72108
	4	0.6664	0.6739	0.67467
	5	0.6304	0.6323	0.63364
	6	0.6032	0.6035	0.60492
	7	0.5918	0.5921	0.59311
	8	0.5992	0.6001	0.60045
	9	0.6257	0.6273	0.62691
α_0 = 60°	2	0.5772	0.6348	0.63423
	3	0.6001	0.6238	0.62361
	4	0.6054	0.6145	0.61459
	5	0.6077	0.6111	0.61128
	6	0.6159	0.6171	0.61721
	7	0.6343	0.6350	0.63479
	8	0.6650	0.6660	0.66525
	9	0.7084	0.7101	0.70873

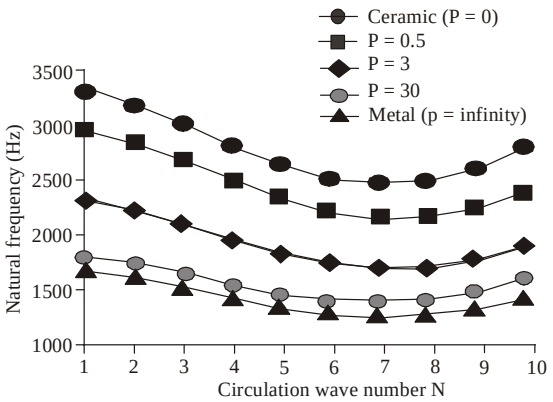

Fig. 4: Natural frequencies associated with various gradient index for the case of semi-vertex cone angle a_0 = 30°, m = 1

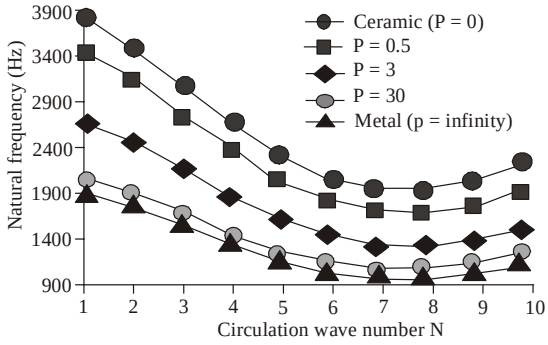

Fig. 5: Natural frequencies associated with various gradient index for the case of semi-vertex cone angle a_0 = 45°, m = 1

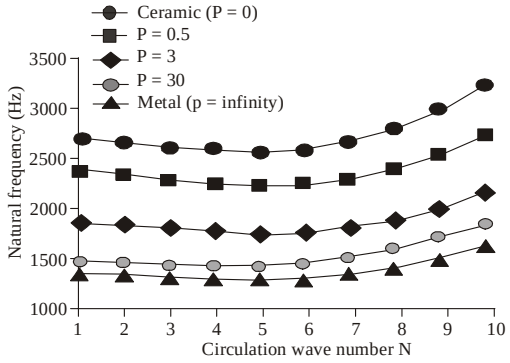

Fig. 6: Natural frequencies associated with various gradient index for the case of semi-vertex cone angle $a_0 = 60^o$, m = 1

E_M = 70 GPa, ρ_M=2710 kg/m^3, μ = 0.3

Ceramic (Almina, Al_2O_3):

E_C=380 GPa,ρ_C = 3800 kg/m^3, μ = 0.3

The variation through the thickness of Young's modulus $E(\eta)$ and mass density per unit volume $\rho(\eta)$ are the same as Eq. (1) and (2). The structural parameters are h = 0.004 m, h/a_2 = 0.01, $(L-L_0)\sin \alpha_0/a_2$ = 0.25. For gradient index p = Infinity, the frequency parameters computed by Eq. (37) are listed in Table 1. Also the corresponding results by Irie *et al*. (1984), Lam and Li (1999) are listed in Table 1.

It is clear from Table 1 that the frequency parameters acquired by the Rayleigh-Ritz method are in good agreement with those in the open literature, which confirms the validity of the present analytical method.

In addition, the principal mode shapes declared by Eq. (29) can be utilized for the conical shells with two simply supported boundaries. In Fig. 4-6, natural frequencies are calculated for the case of semi-vertex cone angles α_0 = 30º, 45º, 60º and gradient index p = 0, 0.5, 3, 30, Infinity and the meridional wave number m = 1.

The forced vibration responses: The forced vibration responses of functionally graded conical shell with two simply supported boundaries are computed. The structural parameters of the functionally graded conical shell sample are identical to those utilized in Section 5.1. The semi-vertex cone angle is $a_0 = 30^o$. The radii at the two ends are a_1 = 0.3m and a_2 = 0.4 m. l_0 = 0.6 m and 1 = 0.8 m are the position coordinates of the conical shell in the curvilinear surface coordinates O-$\xi\zeta\eta$. Thus the length of the conical shell is s = $1-1_0$ = 0.2 m. q_{30} is the amplitude of the impulse loads that equal to 1.0 MPa.

Regarding to Fig. 2, it is assumed that the load applied in the radial direction over a small area:1_2 = 0.01m, $\zeta_1 = 5.062^o$ .The power of exponential pulse is a = 350. For

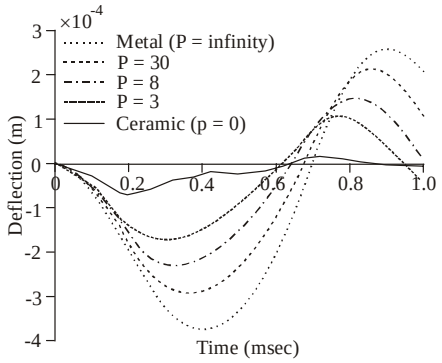

Fig. 7: Time response of center point deflection w under step pulse for various gradient indexes (p)

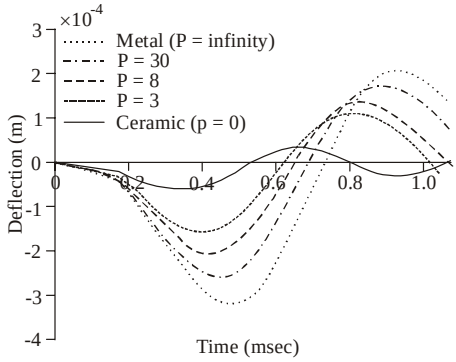

Fig. 8: Time response of center point deflection w under sine pulse for various gradient indexes (p)

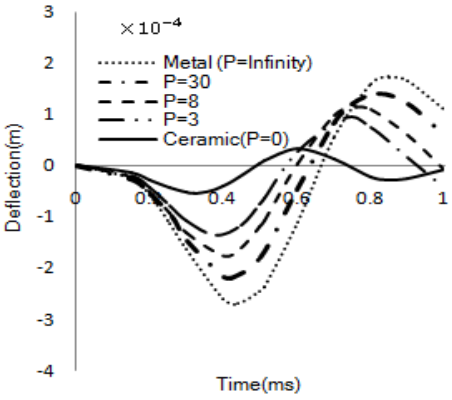

Fig. 9: Time response of center point deflection w under triangular pulse for various gradient indexes (p)

this study, the duration of dynamic loads is chosen same as the natural period of the metal conical shell. The terms of m, n of the Eq. (35) sho choose to converge sufficiently. The number of considered modes (m×n) are as (1×14). The displacement in the η directions of the middle surface of functionally graded conical shell at position $((L+L_0)/2, 0)$ varying with time are shown in

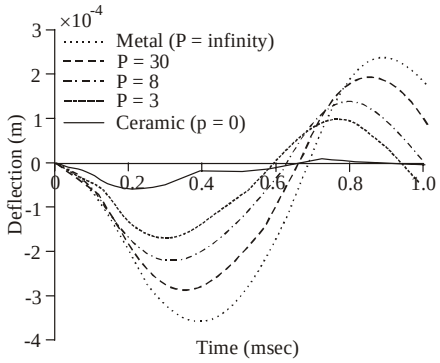

Fig. 10: Time response of center point deflection w under exponential pulse for various gradient indexes (p)

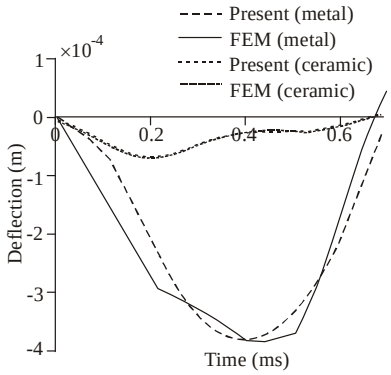

Fig. 11: Comparison of center deflection w under step pulse with ABAQUS

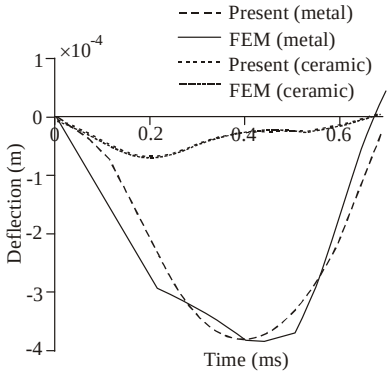

Fig. 12: Comparison of center deflection w under exponential pulse with ABAQUS

Fig. 7-10. From Fig. 11-12, it is observed that the results agree well with the ABAQUS results. At Fig. 13, the finite element model of conical shell under impulse loads is shown.

CONCLUSION

The free vibration and forced vibration of FG conical shell under impulse loads are investigated by using the Rayleigh-Ritz method. For different semi-vertex cone angles a_0 = 30º,45º,60º the natural frequency first decreases and then increases as the circumferential wave number n increases. In all cases when gradient index (p) increases, natural frequencies decrease. The case of P = 0 and a_0 = 30º, conical shell has the highest natural frequencies.

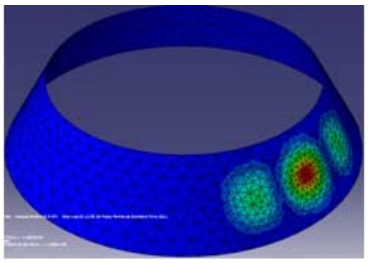

Fig. 13: FEM model for conical shell under impulse loads

The largest deflection happen for metal under step pulse because the area below the load-time curve is greater in comparison with others pulses. When gradient index (p) decreases, the corresponding time response also decreases. The motions of displacement under triangular pulse are similar to the sine pulse.

Appendix : The expressions of the modal mass, modal stiffness and forcing matrices in Eq. (30) are given by:

$$M_1 = \sin\alpha_0 \int_0^{2\pi}\int_{1_0}^{1}\int_{-h/2}^{h/2} UU^T \rho(\eta)\xi d_\eta d_\xi d_\zeta$$

$$M_2 = \sin\alpha_0 \int_0^{2\pi}\int_{1_0}^{1}\int_{-h/2}^{h/2} VV^T \rho(\eta)\xi d_\eta d_\xi d_\zeta$$

$$M_3 = \sin\alpha_0 \int_0^{2\pi}\int_{1_0}^{1}\int_{-h/2}^{h/2} WW^T \rho(\eta)\xi d_\eta d_\xi d_\zeta$$

$$K_1 = \frac{\sin\alpha_0}{1-\mu^2}\int_0^{2\pi}\int_{1_0}^{1}\int_{-h/2}^{h/2}\left(\frac{\partial U}{\partial\xi}\frac{\partial U^T}{\partial\xi}\xi + UU^T\frac{1}{\xi} + \mu\frac{\partial U}{\partial\xi}U^T + \mu U\frac{\partial U^T}{\partial\xi}\right)E(\eta)d_\eta d_\xi d_\zeta + \frac{1}{\sin\alpha_0}\int_0^{2\pi}\int_{10}^{1}\int_{-h/2}^{h/2}\frac{\partial U}{\partial\zeta}\frac{\partial U^T}{\partial\zeta}\frac{1}{\xi}G(\eta)d_\eta d_\xi d_\zeta$$

$$K_2 = \frac{1}{1-\mu^2}\int_0^{2\pi}\int_{1_0}^{1}\int_{-h/2}^{h/2}\left(U\frac{\partial V^T}{\partial\zeta}\frac{1}{\xi} + \mu\frac{\partial U}{\partial\xi}\frac{\partial V^T}{\partial\zeta}\right) E(\eta)d_\eta d_\xi d_\zeta$$

$$+\frac{1}{2(1+\mu)}\int_0^{2\pi}\int_{1_0}^{1}\int_{-h/2}^{h/2}\left(\frac{\partial U}{\partial\zeta}\frac{\partial V^T}{\partial\xi}-\frac{\partial U}{\partial\zeta}V^T\frac{1}{\xi}\right)E(\eta)d_\eta d_\xi d_\zeta$$

$$+\frac{\mu}{(1-\mu^2)\tan\alpha_0}\int_0^{2\pi}\int_{1_0}^{2\pi}\int_{-h/2}^{h/2}\left(\frac{\partial U}{\partial\xi}\right)\left(\frac{\partial V^T}{\partial\zeta}\right)\frac{E(\eta)\eta}{\xi}d_\eta d_\xi d_\zeta$$

$$+\frac{1}{(1-\mu^2)\tan\alpha_0}\int_0^{2\pi}\int_{1_0}^{2\pi}\int_{-h/2}^{h/2}(U)\left(\frac{\partial V^T}{\partial\zeta}\right)\frac{E(\eta)\eta}{\xi^2}d_\eta d_\xi d_\zeta$$

$$+\frac{1}{2(1+\mu)\tan\alpha_0}\int_0^{2\pi}\int_{1_0}^{1}\int_{-h/2}^{h/2}\left(\frac{\partial U}{\partial\zeta}\right)\left(\frac{\partial V^T}{\partial\xi}\right)\frac{E(\eta)\eta}{\xi}d_\eta d_\xi d_\zeta$$

$$-\frac{2}{2(1+\mu)\tan\alpha_0}\int_0^{2\pi}\int_{1_0}^{1}\int_{-h/2}^{h/2}\left(\frac{\partial U}{\partial\zeta}\right)(V^T)\frac{E(\eta)\eta}{\xi^2}d_\eta d_\xi d_\zeta$$

$$K_3=\frac{\cos\alpha_0}{1-\mu^2}\int_0^{2}\int_{10}^{1}\int_{-h/2}^{h/2}\left(UW^T\frac{1}{\xi}+\mu\frac{\partial U}{\partial\xi}W^T\right)E(\eta)d_\eta d_\xi d_\zeta$$

$$-\frac{\sin\alpha_0}{(1-\mu^2)}\int_0^{2\pi}\int_{1_0}^{1}\int_{-h/2}^{h/2}\left(\frac{\partial U}{\partial\xi}\right)\left(\frac{\partial^2 W^T}{\partial\xi^2}\right)E(\eta)\eta\xi d_\eta d_\xi d_\zeta$$

$$-\frac{\sin\alpha_0}{(1-\mu^2)}\int_0^{2\pi}\int_{1_0}^{1}\int_{-h/2}^{h/2}\left(\frac{\partial U}{\partial\xi}\right)\left(\frac{\partial^2 W^T}{\partial\xi^2}\right)E(\eta)\eta\xi d_\eta d_\xi d_\zeta$$

$$-\frac{\mu\sin\alpha_0}{(1-\mu^2)\sin^2\alpha_0}\int_0^{2\pi}\int_{1_0}^{1}\int_{-h/2}^{h/2}\left(\frac{\partial U}{\partial\xi}\right)\left(\frac{\partial^2 W^T}{\partial\varsigma^2}\right)\frac{E(\eta)\eta}{\xi}d\eta d\xi d\zeta$$

$$-\frac{\mu\sin\alpha_0}{(1-\mu^2)\sin^2\alpha_0}\int_0^{2\pi}\int_{1_0}^{1}\int_{-h/2}^{h/2}\left(\frac{\partial U}{\partial\xi}\right)\left(\frac{\partial^2 W^T}{\partial\varsigma^2}\right)\frac{E(\eta)\eta}{\xi}d\eta d\xi d\zeta$$

$$-\frac{\mu\sin\alpha_0}{(1-\mu^2)}\int_0^{2\pi}\int_{1_0}^{1}\int_{-h/2}^{h/2}\left(\frac{\partial U}{\partial\xi}\right)\left(\frac{\partial W^T}{\partial\xi}\right)E(\eta)\eta d_\eta d_\xi d_\zeta$$

$$-\frac{1}{(1-\mu^2)\sin\alpha_0}\int_0^{2\pi}\int_{10}^{1}\int_{-h/2}^{h/2}(U)\left(\frac{\partial^2 W^T}{\partial\zeta^2}\right)\frac{E(\eta)\eta}{\xi^2}d_\eta d_\xi d_\zeta$$

$$-\frac{\sin\alpha_0}{(1-\mu^2)}\int_0^{2\pi}\int_{10}^{1}\int_{-h/2}^{h/2}(U)\left(\frac{\partial W^T}{\partial\xi}\right)\frac{E(\eta)\eta}{\xi}d_\eta d_\xi d_\zeta$$

$$-\frac{\mu\sin\alpha_0}{(1-\mu^2)}\int_0^{2\pi}\int_{0}^{1}\int_{-h/2}^{h/2}(U)\left(\frac{\partial^2 W^T}{\partial\xi^2}\right)E(\eta)\eta d_\eta d_\xi d_\zeta$$

$$-\frac{2}{2(1+\mu)\sin\alpha_0}\int_0^{2\pi}\int_{1_0}^{1}\int_{-h/2}^{h/2}\left(\frac{\partial U}{\partial\zeta}\right)\left(\frac{\partial^2 W^T}{\partial\xi\partial\zeta}\right)\frac{E(\eta)\eta}{\xi}d_\eta d_\xi d_\zeta$$

$$+\frac{2}{2(1+\mu)\sin\alpha_0}\int_0^{2\pi}\int_{1_0}^{1}\int_{-h/2}^{h/2}\left(\frac{\partial U}{\partial\zeta}\right)\left(\frac{\partial W^T}{\partial\zeta}\right)\frac{E(\eta)\eta}{\xi^2}d_\eta d_\xi d_\zeta$$

$$K_4=\frac{1}{(1-\mu^2)\sin\alpha_0}$$

$$\int_0^{2\pi}\int_0^{1}\int_{-h/2}^{h/2}\left(\frac{\partial V}{\partial\zeta}\frac{\partial V^T}{\partial\zeta}\frac{1}{\xi}+\frac{\eta^2}{\tan^2\alpha_0}\frac{\partial v}{\partial\zeta}\frac{\partial V^T}{\partial\zeta}\frac{1}{\xi^3}\right)E(\eta)d_\eta d_\xi d_\zeta+\sin\alpha_0\times$$

$$\int_0^{2\pi}\int_0^{1}\int_{-h/2}^{h/2}\left(\frac{\partial V}{\partial\xi}\frac{\partial V^T}{\partial\xi}\xi+VV^T\frac{1}{\xi}\right.$$

$$\left.-\frac{\partial V}{\partial\xi}V^T-V\frac{\partial V^T}{\partial\xi}\right)G(\eta)d_\eta d_\xi d_\zeta+\frac{\sin\alpha_0}{\tan^2\alpha_0}\times$$

$$\int_0^{2\pi}\int_{1_0}^{1}\int_{-h/2}^{h/2}\left(VV^T\frac{1}{\xi}\right)G(\eta)d_\eta d_\xi d_\zeta+$$

$$\int_0^{2\pi}\int_{1_0}^{1}\int_{-h/2}^{h/2}\eta^2\left(\frac{\partial V}{\partial\xi}\frac{\partial V^T}{\partial\xi}\frac{1}{\xi}+4VV^T\frac{1}{\xi^3}\right)G(\eta)d_\eta d_\xi d_\zeta+$$

$$\int_0^{2\pi}\int_{1_0}^{1}\int_{-h/2}^{h/2}\eta^2\left(-2\frac{\partial V}{\partial\xi}V^T\frac{1}{\xi^2}-2V\frac{\partial V^T}{\partial\xi}\frac{1}{\xi^2}\right)$$
$$G(\eta)d_\eta d_\xi d_\zeta +$$
$$\frac{2}{(1-\mu^2)\sin\alpha_0\tan\alpha_0}\int_0^{2}\int_{1_0}^{1}\int_{-h/2}^{h/2}\left(\frac{\partial V}{\partial\zeta}\right)\left(\frac{\partial V^T}{\partial\zeta}\right)$$
$$\frac{E(\eta)\eta}{\xi^2}d_\eta d_\xi d_\zeta$$
$$+\frac{2\cos\alpha_0}{2(1+\mu)}\int_0^{2\pi}\int_{1_0}^{1}\int_{-h/2}^{h/2}\left(\frac{\partial V}{\partial\xi}\right)\left(\frac{\partial V^T}{\partial\xi}\right)E(\eta)\eta d_\eta d_\xi d_\zeta$$

$$-\frac{3\cos\alpha_0}{2(1+\mu)}\int_0^{2\pi}\int_{1_0}^{1}\int_{-h/2}^{h/2}\left(\frac{\partial V}{\partial\xi}\right)(V^T)\frac{E(\eta)\eta}{\xi}d_\eta d_\xi d_\zeta$$

$$-\frac{3\cos\alpha_0}{2(1+\mu)}\int_0^{2\pi}\int_{1_0}^{1}\int_{-h/2}^{h/2}(V)\left(\frac{\partial V^T}{\partial\xi}\right)\frac{E(\eta)\eta}{\xi}d_\eta d_\xi d_\zeta$$

$$+\frac{4\cos\alpha_0}{2(1+\mu)}\int_0^{2\pi}\int_{1_0}^{1}\int_{-h/2}^{h/2}(V)\left(V^T\right)\frac{E(\eta)\eta}{\xi^2}d_\eta d_\xi d_\zeta$$

$$K_5=\frac{1}{(1-\mu^2)\tan\alpha_0}\int_0^{2\pi}\int_{1_0}^{1}\int_{-h/2}^{h/2}\frac{\partial V}{\partial\zeta}\frac{w^T}{\xi}$$
$$E(\eta)d_\eta d_\xi d_\zeta$$

$$-\frac{1}{(1-\mu^2)\tan\alpha_0}\int_0^{2\pi}\int_{1_0}^{1}\int_{-h/2}^{h/2}(\frac{\partial V}{\partial\zeta}\frac{\partial W^T}{\partial\xi}\frac{1}{\xi^2}+$$
$$\mu\frac{\partial V}{\partial\zeta}\frac{\partial^2W^T}{\partial\xi^2}\frac{1}{\xi}+\frac{1}{\sin^2\alpha_0}\frac{\partial v}{s\partial\zeta}\frac{\partial^2W^T}{\partial\zeta^2}\frac{1}{\xi^3})$$
$$E(\eta)\eta^2d_\eta d_\xi d_\zeta +$$

$$\frac{2}{\tan\alpha_0}\int_0^{2}\int_{1_0}^{1}\int_{-h/2}^{h/2}\left(\frac{\partial V}{\partial\xi}\frac{\partial W^T}{\partial\zeta}\frac{1}{\xi^2}\right.$$
$$-\frac{\partial V}{\partial\xi}\frac{\partial^2W^T}{\partial\xi\partial\zeta}\frac{1}{\xi}+\frac{2V}{\xi^2}\frac{\partial^2W^T}{\partial\xi\partial\zeta}-$$

$$\left.\frac{2V}{\xi^3}\frac{\partial W^T}{\partial\zeta}\right)G(\eta)\eta^2d_\eta d_\xi d_\zeta+\frac{1}{(1-\mu^2)\tan^2\alpha_0}\times$$

$$\int_0^{2\pi}\int_{1_0}^{1}\int_{-h/2}^{h/2}\left(\frac{\partial V}{\partial\zeta}\right)(W^T)\frac{E(\eta)\eta}{\xi^2}d_\eta d_\xi d_\zeta$$

$$-\frac{1}{(1-\mu^2)\sin^2\alpha_0}\int_0^{2\pi}\int_{10}^{1}\int_{-h/2}^{h/2}\left(\frac{\partial V}{\partial\zeta}\right)\left(\frac{\partial^2W^T}{\partial\zeta^2}\right)$$
$$\frac{E(\eta)\eta}{\xi^2}d_\eta d_\xi d_\zeta$$

$$-\frac{1}{(1-\mu^2)}\int_0^{2\pi}\int_{10}^{1}\int_{-h/2}^{h/2}\left(\frac{\partial V}{\partial\zeta}\right)\left(\frac{\partial W^T}{\partial\xi}\right)$$
$$\frac{E(\eta)\eta}{\xi}d_\eta d_\xi d_\zeta$$

$$-\frac{\mu}{(1-\mu^2)}\int_0^{2\pi}\int_{1_0}^{1}\int_{-h/2}^{h/2}\left(\frac{\partial V}{\partial\zeta}\right)\left(\frac{\partial^2W^T}{\partial\xi^2}\right)E(\eta)\eta d_\eta d_\xi d_\zeta$$

$$-\frac{2}{2(1+\mu)}\int_0^{2\pi}\int_{1_0}^{1}\int_{-h/2}^{h/2}\left(\frac{\partial V}{\partial\xi}\right)\left(\frac{\partial^2W^T}{\partial\xi\partial\zeta}\right)E(\eta)\eta d_\eta d_\xi d_\zeta$$

$$+\frac{2}{2(1+\mu)\sin\alpha_0}\int_0^{2\pi}\int_{1_0}^{1}\int_{-h/2}^{h/2}\left(\frac{\partial V}{\partial\xi}\right)\left(\frac{\partial W^T}{\partial\zeta}\right)$$
$$\frac{E(\eta)\eta}{\xi^2}d_\eta d_\xi d_\zeta$$

$$+\frac{2}{2(1+\mu)}\int_0^{2\pi}\int_{1_0}^{1}\int_{-h/2}^{h/2}\quad(V)\left(\frac{\partial^2W^T}{\partial\xi\partial\zeta}\right)$$
$$\frac{E(\eta)\eta}{\xi}d_\eta d_\xi d_\zeta$$

$$-\frac{2}{2(1+\mu)}\int_0^{2\pi}\int_{1_0}^{1}\int_{-h/2}^{h/2}(V)\left(\frac{\partial W^T}{\partial\zeta}\right)\frac{E(\eta)\eta}{\xi^2}d_\eta d_\xi d_\zeta$$

$$K_6=\frac{\sin\alpha_0}{(1-\mu^2)}\int_0^{2\pi}\int_{1_0}^{1}\int_{-h/2}^{h/2}(\frac{\partial^2w}{\partial\xi^2}\frac{\partial^2w^T}{\partial\xi^2}\xi$$
$$+\frac{\partial w}{\partial\xi}\frac{\partial w^T}{\partial\xi}\frac{1}{\xi}+\mu\frac{\partial^2w}{\partial\xi^2}\frac{\partial w^T}{\partial\xi}+\mu\frac{\partial w}{\partial\xi}\frac{\partial^2w^T}{\partial\xi^2})$$
$$E(\eta)\eta^2d_\eta d_\xi d_\zeta$$

$$+\frac{1}{(1-\mu^2)\sin\alpha_0}\int_0^{2\pi}\int_{1_0}^{1}\int_{-h/2}^{h/2}(\frac{1}{\sin^2\alpha_0}\frac{\partial^2w}{\partial\zeta^2}\frac{\partial^2w^T}{\partial\zeta^2}\frac{1}{\xi^3}$$
$$+\mu\frac{\partial^2w}{\partial\xi^2}\frac{\partial^2w^T}{\partial\zeta^2}\frac{1}{\xi}+\mu\frac{\partial^2w}{\partial\zeta^2}\frac{\partial^2w^T}{\partial\xi^2}\frac{1}{\xi}+\frac{\partial^2w}{\partial\zeta^2}\frac{\partial w^T}{\partial\xi}\frac{1}{\xi^2}$$
$$+\frac{\partial w}{\partial\xi}\frac{\partial^2w^T}{\partial\zeta^2}\frac{1}{\xi^2})E(\eta)\eta^2d_\eta d_\xi d_\zeta$$

$$+\frac{\sin\alpha_0}{\left(1-\mu^2\right)\tan^2\alpha_0}\int_0^{2\pi}\int_{1_0}^{1}\int_{-h/2}^{h/2}\frac{ww^T}{\xi}E(\eta)d_\eta d_\xi d_\zeta +$$

$$\frac{4}{\sin\alpha_0}\int_0^{2\pi}\int_{1_0}^{1}\int_{-h/2}^{h/2}(\frac{\partial^2w}{\partial\xi\partial\zeta}\frac{\partial^2w^T}{\partial\xi\partial\zeta}\xi+\frac{\partial w}{\partial\zeta}\frac{\partial w^T}{\partial\zeta}\frac{1}{\xi}$$
$$-\frac{\partial^2w}{\partial\xi\partial\zeta}\frac{\partial w^T}{\partial\zeta}-\frac{\partial w}{\partial\zeta}\frac{\partial^2w^T}{\partial\xi\partial\zeta})\frac{G(\eta)}{\xi^2}\eta^2d_\eta d_\xi d_\zeta -$$
$$\frac{1}{(1-\mu^2)\sin\alpha_0\tan\alpha_0}\int_0^{2\pi}\int_{1_0}^{1}\int_{-h/2}^{h/2}(\frac{\partial^2w}{\partial\zeta^2})$$
$$\left(W^T\right)\frac{E(\eta)\eta}{\xi^2}d_\eta d_\xi d_\zeta$$

$$-\frac{\cos\alpha_0}{\left(1-\mu^2\right)}\int_0^{2\pi}\int_{1_0}^{1}\int_{-h/2}^{h/2}\left(\frac{\partial W}{\partial\xi}\right)\left(W^T\right)\frac{E(\eta)\eta}{\xi}d_\eta d_\xi d_\zeta$$

$$-\frac{\mu\cos\alpha_0}{\left(1-\mu^2\right)}\int_0^{2\pi}\int_{1_0}^{1}\int_{-h/2}^{h/2}\left(\frac{\partial^2 W}{\partial\xi^2}\right)\left(W^T\right)E(\eta)\eta d_\eta d_\xi d_\zeta$$

$$-\frac{1}{\left(1-\mu^2\right)\sin\alpha_0\tan\alpha_0}\int_0^{2\pi}\int_{10}^{1}\int_{-h/2}^{h/2}(W)\left(\frac{\partial^2 W^T}{\partial\zeta^2}\right)\frac{E(\eta)\eta}{\xi^2}$$
$$d_\eta d_\xi d_\zeta$$

$$-\frac{\cos\alpha_0}{\left(1-\mu^2\right)}\int_0^{2\pi}\int_{1_0}^{1}\int_{-h/2}^{h/2}(W)\left(\frac{\partial W^T}{\partial\xi}\right)\frac{E(\eta)\eta}{\xi}d_\eta d_\xi d_\zeta$$

$$-\frac{\mu\cos\alpha_0}{\left(1-\mu^2\right)}\int_0^{2\pi}\int_{1_0}^{1}\int_{-h/2}^{h/2}(W)\left(\frac{\partial^2 W^T}{\partial\xi^2}\right)E(\eta)\eta d_\eta d_\xi d_\zeta$$

$$F_{q3}=\sin\alpha_0\int_{-\zeta_1}^{\zeta_1}\int_{\frac{L+L_0}{2}-1_2}^{\frac{L+L_0}{2}+1_2}W^T\xi d_\xi d_\zeta \qquad (38)$$

REFERENCES

Christoforou, A.P. and S.R. Swanson, 1990. Analysis of simply-supported orthotropic cylindrical shells subjected to lateral impact loads. J. Appl. Mech., 57: 376-383.

Clough, R.W. and J. Penzien, 1993. Dynamics of Structures. 2nd Edn., McGraw-Hill Inc., New York.

Fares, M.E. and Y.G. Youssif and A.E. Alamir, 2004. Design and control optimization of composite laminated truncated conical shells for minimum dynamic response including transverse shear deformation. Compos. Struct., 64: 139-150.

Irie, T. and G. Yamada and K. Tanaka, 1984. Natural frequencies of truncated conical shells. J. Sound Vib., 92: 447-453.

Jafari, A.A. and S.M.R. Khalili and R. Azarafza, 2005. Transient dynamic response of composite circular cylindrical shells under radial impulse load and axial compressive loads. Thin-Wall. Struct., 43(11): 1763-1786.

Kandasamy, S., 2008. Vibration analyses of open shells of revolution. Ph.D. Thesis, University of Western Ontario.

Khalili, S.M.R., R. Azarafza and A. Davar, 2009. Transient dynamic response of initially stressed composite circular cylindrical shells under radial impulse load. Compos. Struct., 89: 275-284.

Kieback, B., A. Neubrand and H. Riedel, 2003. Processing techniques for functionally graded materials. Mater. Sci. Eng. A, 362: 81-105.

Lam, K.Y. and H. Li, 1999. Influence of boundary conditions on the frequency characteristics of a rotating truncated circular conical shell. J. Sound Vib., 223: 171-195.

Lee, Y.S. and K.D. Lee, 1997. On the dynamic response of laminated circular cylindrical shells under impulse loads. Comput. Struct., 63(1): 149-157.

Li, H., 2000. Frequency analysis of rotating truncated circular orthotropic conical shells with different boundary conditions. Composites Sci. Tech., 60: 2945-55.

Liew, K.M., X.Q. He, T.Y. Ng and S. Kitipornchai, 2002. Active control of FGM shell subjected to a temperature gradient via piezoelectric sensor/actuator patches. Int. J. Numer. Meth. Engng., 55: 653-668.

Malekzadeh, K., S.M.R. Khalili and A. Davar and P. Mahajan, 2010. Transient dynamic response of clamped-free hybrid composite circular cylindrical shells. Appl. Compos. Mater., 17: 243-57.

Matemilola, S.A. and W.J. Stronge, 1997. Impact response of composite cylinders. Int. J. Solids Struct., 34(21): 2669-2684.

Matsunaga, H., 2009. Free vibration and stability of functionally graded circular cylindrical shell according to a 2D higher-order shear deformation theory. Compos. Struct., 88: 519-531.

Miyamoto, Y., W.A. Kaysser and B.H. Rabin and A. Kawasaki and R.G. Ford, 1999. Functionally Graded Materials: Design, Processing and Applications. Kluwer Academic Publishers, London.

Obata Y. and N. Noda, 1996. Optimum material design for functionally gradient material plate. Arch. Appl. Mech., 66: 581-589.